

# Roddie et al. Supplementary Information

## Supplementary methods

### Analysis of macrophage morphology

Macrophage morphology was assessed using Fiji by manually selecting (polygon selection tool) individual macrophages on the ventral midline that could be easily discriminated from their neighbours and were fully in the field of view. Area, perimeter and shape descriptor measurements were selected for analysis. Circularity is defined by the equation  $4\pi \times (\text{area}/\text{perimeter}^2)$ . A value of 1.0 indicates a perfect circle, with cells becoming increasingly long as this ratio approaches zero.

### Imaging and analysis of wounding-induced calcium waves

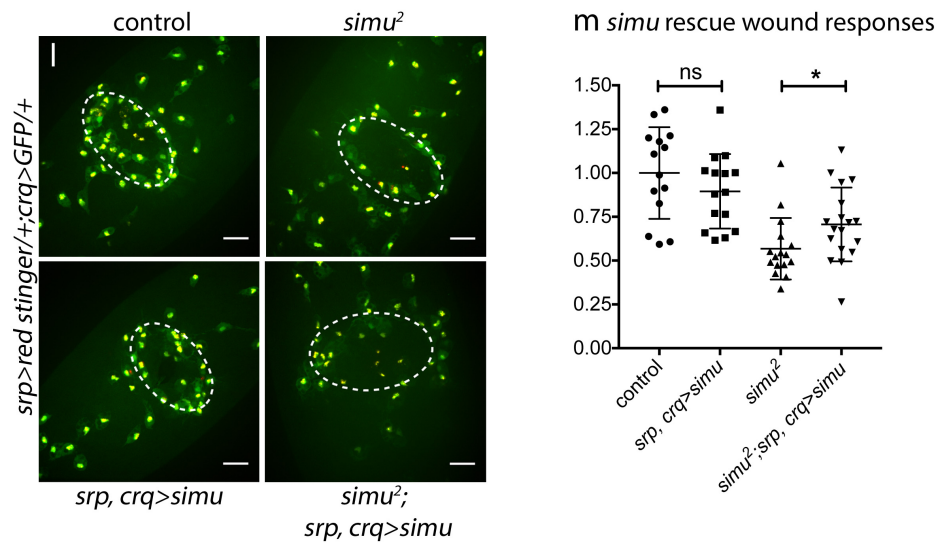
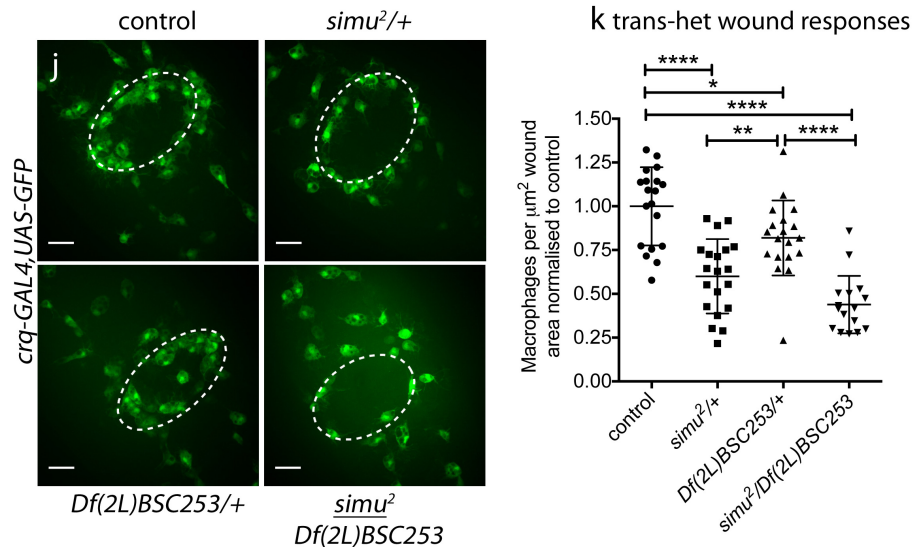
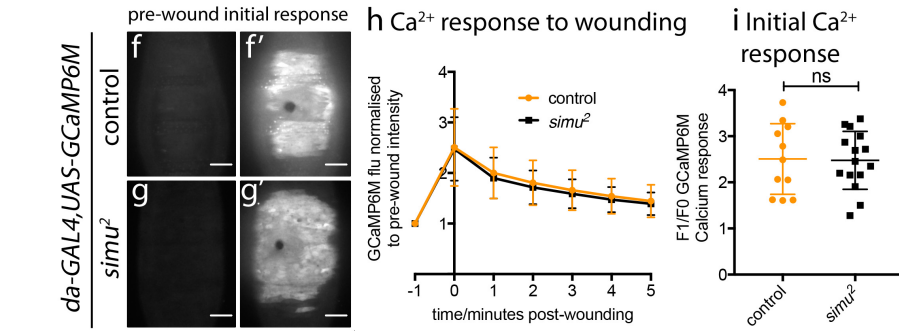
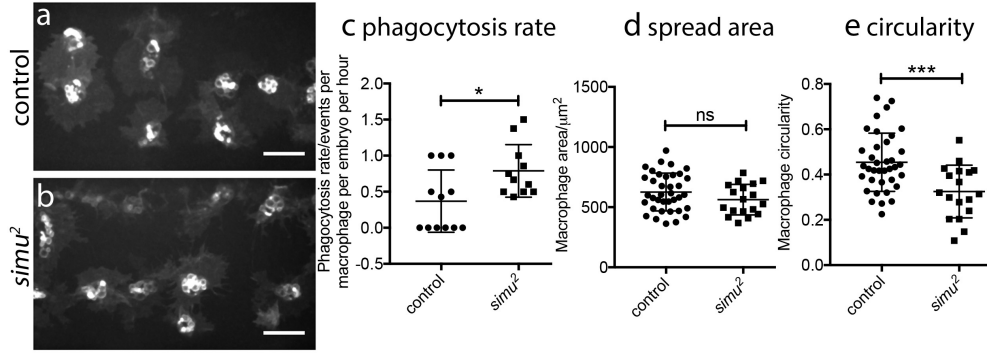
The epithelia of embryos expressing the cytosolic calcium reporter GCaMP6M were imaged before and after wounding. Z-stacks were taken every 15 seconds for 5 minutes to show calcium responses to wounding and subsequent calcium dynamics. Pre-wound and wounding movies were concatenated in Fiji and maximum projections made. The mean gray value (MGV) of GCaMP6M fluorescence was measured within the area bounded by the vitelline membrane (selected using the polygon selection tool) for each projection time-point and the F1/F0 ratio calculated (F1 is the fluorescence at a particular time-point; F0 is the pre-wound fluorescence).

### Quantification of caspase reporter activity

Embryos expressing a caspase reporter (apoliner) were imaged live on their ventral surface 60-minutes after heat-shock treatment (0, 15 or 30 minutes). Maximum projections were assembled in Fiji and a registration plugin (stack reg) used to minimise drift. Images were cropped to a 100µm x 90µm region of interest, corresponding to the two most-medial abdominal segments. The cumulative numbers of GFP-positive nuclei per field of view was assessed (n=3 per condition). These experiments formed the basis for selecting the 15-minute heat-shock condition and wounding at 60-minutes post-heat shock. Under these conditions and at this timepoint, cells exhibit caspase activity and are destined to undergo apoptosis, but have yet to delaminate and be removed by efferocytosis.

## Supplementary Figures

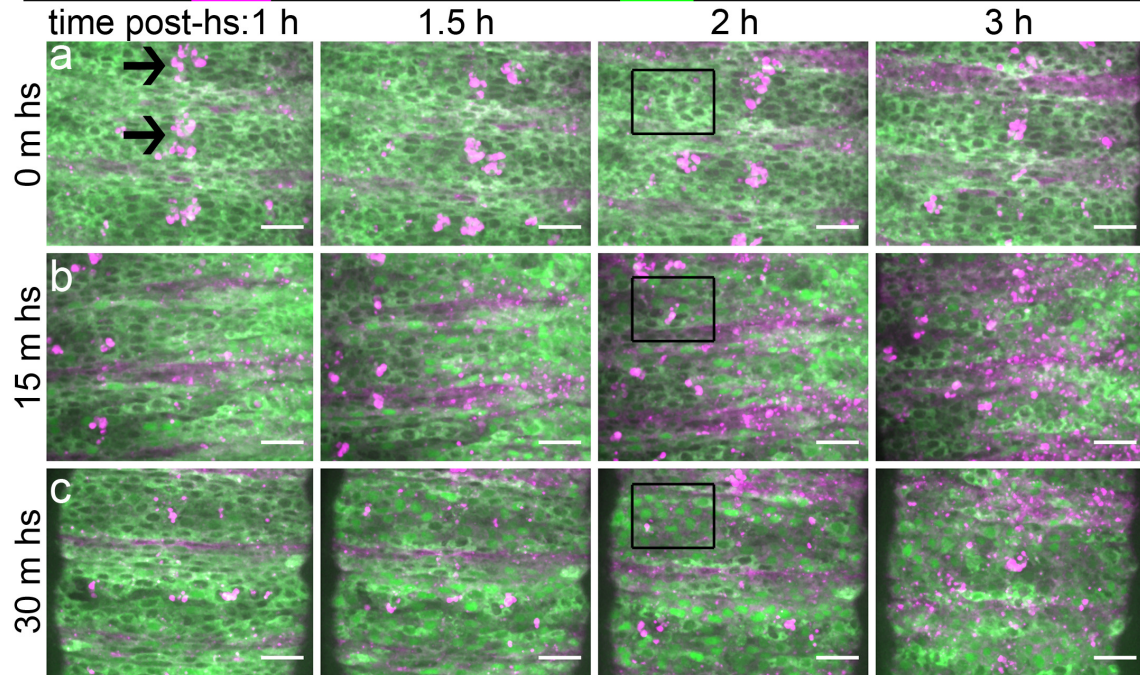
*crq-GAL4,UAS-CD4-tdTomato*



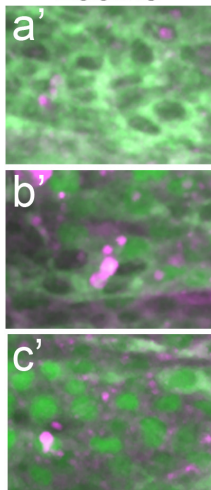
## Supplementary Figure 1 - *simu* has a partially cell autonomous function in macrophages and generation of wound signals are normal in the absence of *simu*

(a) ventral images showing macrophage morphology in control (*w;;crq-GAL4,UAS-CD4-tdTomato*) and *simu* mutant embryos (*w;simu<sup>2</sup>;crq-GAL4,UAS-CD4-tdTomato*) at stage 15. (c-e) scatterplots showing rates of phagocytosis (phagocytic events per hour, per macrophage, per embryo, c), macrophage spread area ( $\mu\text{m}^2$  per macrophage, d) and macrophage circularity (e). Statistical comparisons made via Mann-Whitney tests; n=12 control and 11 *simu<sup>2</sup>* embryos (c) and n=37 control and 18 *simu<sup>2</sup>* macrophages taken from 11 embryos (d-e). p=0.028, 0.179, 0.0009 (c-e). (f-g) images of the calcium flash (visualised using GCaMP6M) in the epithelium prior to (f-g) and immediately after wounding (f'-g') in control (*w;;da-GAL4,UAS-GCaMP6M*, f-f') and *simu* mutant embryos (*w;simu<sup>2</sup>;da-GAL4,UAS-GCaMP6M*, g-g'). (h) line graph showing timecourses of GCaMP6M response (GCaMP6M mean gray value (MGV) of the entire embryonic field of view at each timepoint normalised to the pre-wound MGV) in control and *simu* mutant embryos (same genotypes as f-g). (i) scatterplot of the ratio of initial response (F1) and pre-wound (F0) MGV in control and *simu* mutant embryos (n=11 and 15, respectively; p=0.80, Mann-Whitney test). (j) ventral images showing wound responses in control (*w;;crq-GAL4,UAS-GFP*), *simu*/+ heterozygous (*w;simu<sup>2</sup>/+;crq-GAL4,UAS-GFP*), *Df(2L)BSC253*/+ heterozygous (*w;Df(2L)BSC253/+;crq-GAL4,UAS-GFP*) and *simu*/*Df(2L)BSC253* trans-heterozygous embryos (*w;simu<sup>2</sup>/Df(2L)BSC253;crq-GAL4,UAS-GFP*) at 60-minutes post-wounding. (k) scatterplot showing wound responses corresponding to genotypes shown in (j). N numbers (left-right) are 19, 20, 19, 16; ns, \*, \*\*, \*\*\* and \*\*\*\* denote not significant (p=0.10), p=0.043, 0.0079 and p<0.0001, respectively, via one-way ANOVA with Dunn's multiple comparisons post-test. (l) ventral images showing wound responses (macrophages per wound area, normalised to control) at 60-minutes post-wounding in controls (*w;srp-GAL4,UAS-red stinger/+;crq-GAL4,UAS-GFP/+*), *simu* mutants (*w;simu<sup>2</sup>,srp-GAL4,UAS-red stinger/simu<sup>2</sup>;crq-GAL4,UAS-GFP/+*), embryos in which *simu* was re-expressed in macrophages (*w;srp-GAL4,UAS-red stinger/+;crq-GAL4,UAS-GFP/UAS-simu*) and *simu* mutants in which *simu* was re-expressed in macrophages (*w;simu<sup>2</sup>,srp-GAL4,UAS-red stinger/simu<sup>2</sup>;crq-GAL4,UAS-GFP/UAS-simu*). (m) scatterplot showing wound responses corresponding to genotypes in (l). N numbers (left-right) are 14, 15, 16, 18; ns and \* denote not significant (p=0.27) and p=0.017, via Mann-Whitney tests. Lines and error bars represent mean and standard deviation on scatterplots; scale bars indicate 20 $\mu\text{m}$ .

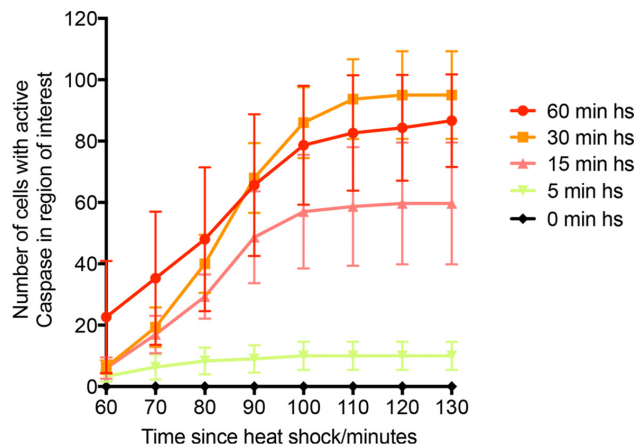
*da>apoliner* (purple=membrane-tethered RFP; green=nls-GFP released by caspase activity)



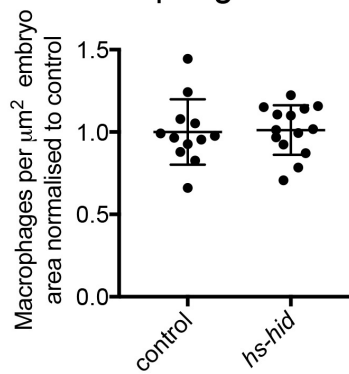
zooms



d timecourse of caspase activation

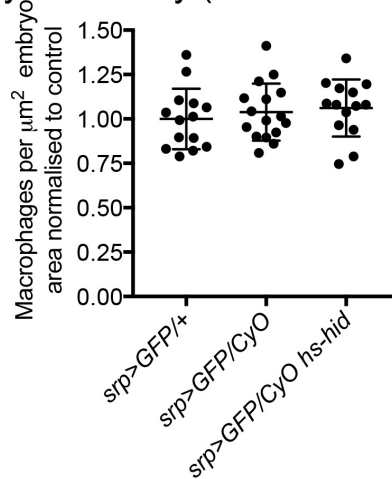


e pre-wound macrophage density

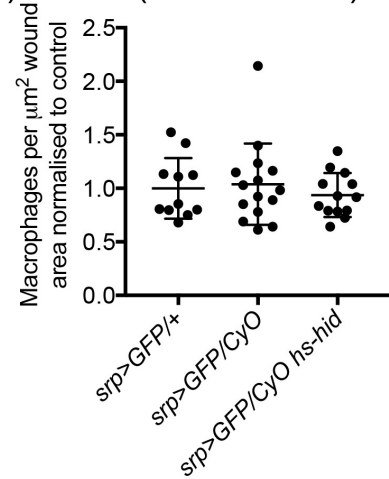


corresponds to data from Fig. 5 wounds

f pre-wound macrophage density (no hs control)



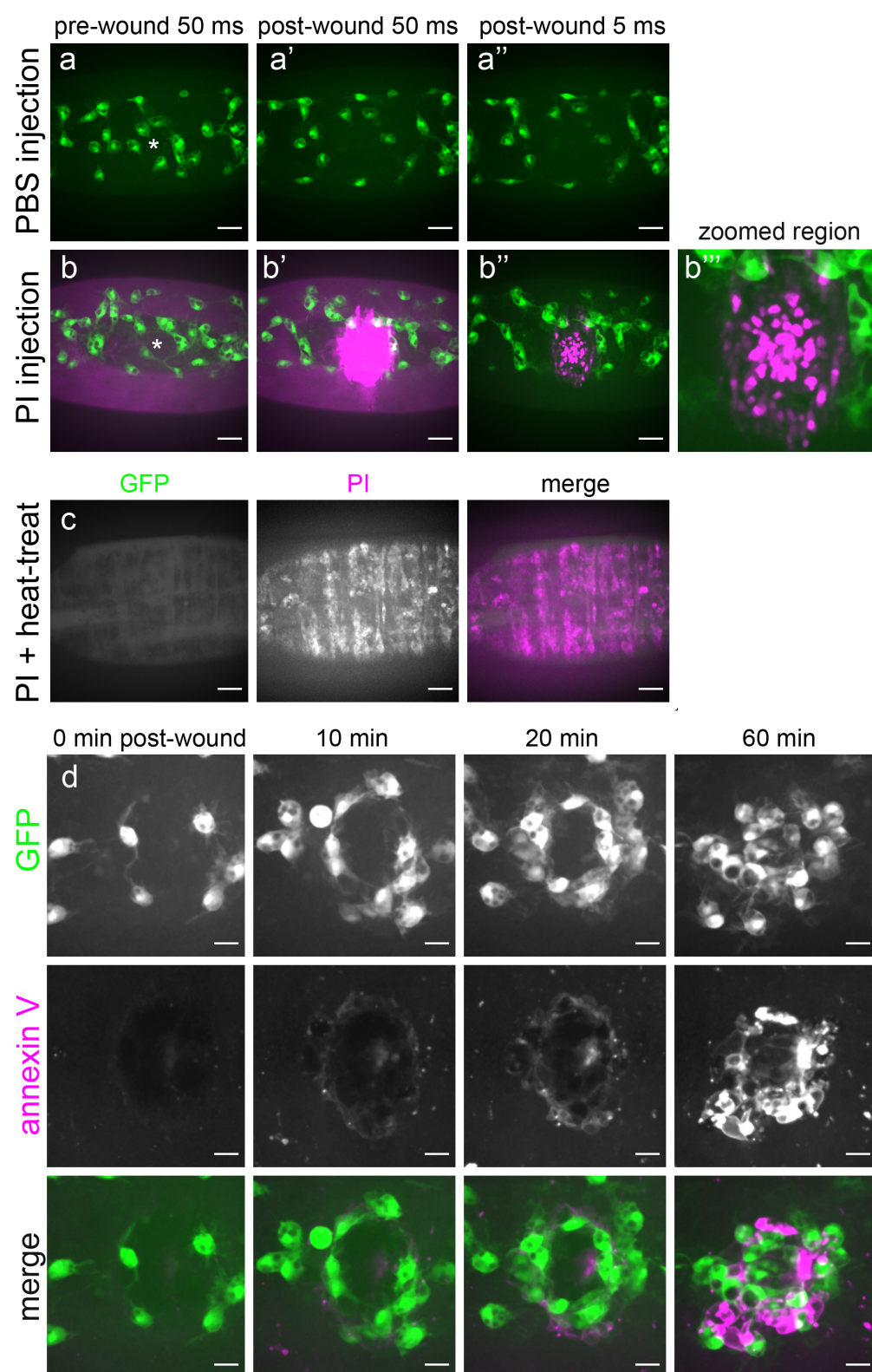
g wound response (no hs control)



## Supplementary Figure 2 - Characterisation of induction of apoptosis using *hs-hid* and heat-shock of embryos

(a-c) embryos ubiquitously expressing a caspase reporter and carrying the *hs-hid* transgene (*w;CyO hs-hid/+;da-GAL4,UAS-apoliner/+*) were heat-shocked for 0, 15 or 30 minutes and imaged from 60-minutes post heat-shock. Relocalisation of nls-GFP (green) from membranes (via a CD8-RFP tether, purple) to the nucleus following caspase-dependent cleavage between these two fluorophores denotes cells in which caspases are active. Projections show ventral side of embryos at indicated times after heat-shock; arrows indicate examples of macrophages with RFP-positive “historical” phagosomes; boxes show regions shown at higher magnification in (a'-c'). (d) quantification of rate of generation of caspase-positive cells (cumulative numbers of GFP-positive nuclei over time) following heat-shock (shows mean of n=3 per condition  $\pm$  standard error of the mean). (e) scatterplot showing density of macrophages (macrophages per  $\mu\text{m}^2$  embryo area, normalised to the mean of the control) on the ventral midline immediately prior to wounding in control and *hs-hid* embryos (n=12 and 14, respectively; p=0.527, Mann-Whitney test); this pre-wound data corresponds to wounded embryo data set shown in Fig. 5. (g-f) scatterplots of data from control experiments to address whether genetic background, rather than induction of apoptosis, accounted for the impairment of wound responses seen in Fig. 5: stage 15 *w;srp-GAL4,UAS-GFP/+*, *w;srp-GAL4,UAS-GFP/CyO* and *w;srp-GAL4,UAS-GFP/CyO hs-hid* embryos were wounded without heat-shock treatment. There was no difference in pre-wound macrophage density (n=14, 16, 14, respectively, g) or wound responses between genotypes (n=11, 15, 13, respectively, f), indicating that neither the presence of a balancer chromosome (*CyO*) nor the *hs-hid* transgenic insertion affected either developmental dispersal or recruitment to wounds. Statistical analysis via one-way ANOVA with Tukey's multiple comparison test (f-g); p values for (f-g) are as follows: *srp>GFP/+* vs. *srp>GFP/CyO* p=0.80 (f); p=0.95 (g); *srp>GFP/+* vs. *srp>GFP/CyO hs-hid* p=0.59 (f); p=0.87 (g); *srp>GFP/CyO* vs. *srp>GFP/CyO hs-hid* p=0.92 (f); p=0.66 (g). Lines and error bars represent mean and standard deviation in scatterplots; scale bars indicate 20 $\mu\text{m}$  in image panels.





## Supplementary Fig. 3 - Laser-induced injury results in presentation of phosphatidylserine and membrane rupture with large amounts of non-apoptotic debris persisting at wound sites

**(a-b)** PBS **(a)** or propidium iodide (PI) injected **(b)** stage 15 embryos with GFP-labelled macrophages (*w;;crq-GAL4,UAS-GFP*) were imaged before and immediately after wounding, showing a dramatic accumulation of PI staining at the wound site immediately after laser-mediated ablation. Timings refer to exposure duration during image capture - a shorter exposure time (5 ms) reveals detail of nuclear localisation of PI, suggestive of necrotic cell death **(b'')**; zoomed panel **(b''')** shows close up of wound region in **(b'')**. **(c)** as a positive control, embryos of the same genotype were heat treated for 15 minutes at 60°C, resulting in widespread entry of PI into cells and leakage of GFP from macrophages. **(d-d')** injection of texas red-labelled annexin V (as a marker for phosphatidylserine (PS)) into the vitelline space of stage 15 embryos with GFP-labelled macrophages (*w;;crq-GAL4,UAS-GFP*) reveals a rapid and sustained accumulation of annexin V at the wound edge and within the wound, including on cells in the process of being engulfed by those macrophages that have migrated to that site. Scale bars represent 20µm **(a-c)** and 10µm **(d)**.

## Supplementary Tables

### Supplementary Table 1 - Fly genotypes used in this study

Figure	Abbreviation used	Full genotype	Source (indicated for first panel in which allele/transgene used)
Fig. 1a	control	w[1118];srp-GAL4,UAS-GFP	srp-GAL4,UAS-GFP obtained from Will Wood, University of Edinburgh
Fig. 1b	DI(3L)H99	w[1118];srp-GAL4,UAS-GFP,DI(3L)H99	DI(3L)H99 obtained from Bloomington Stock Centre and recombined to remove mapping markers
Fig. 1c, g-h	control	w[1118];crq-GAL4,UAS-GFP	crq-GAL4,UAS-GFP obtained from Will Wood, University of Edinburgh
Fig. 1e, g-h	DI(3L)H99	w[1118];DI(3L)H99,crq-GAL4,UAS-GFP	
Fig. 1i-l, n	control	w[1118];srp-GAL4,UAS-2xFYVE-GFP,crq-GAL4,UAS-CD4-tdTomato	UAS-2xFYVE-GFP and UAS-CD4-tdTomato obtained from Bloomington Stock Centre
Fig. 1k, m-n	DI(3L)H99	w[1118];srp-GAL4,UAS-2xFYVE-GFP,DI(3L)H99,crq-GAL4,UAS-CD4-tdTomato	
Fig. 2a-d	control	w[1118];srp-GAL4,UAS-GFP/+crq-GAL4,UAS-GFP/+	
Fig. 2e, g-h	control	w[1118];crq-GAL4,UAS-GFP	
Fig. 2i-h	simu[2]	w[1118];simu[2];crq-GAL4,UAS-GFP	simu[2] obtained from Estee Kurant, University of Haifa
Fig. 3	control	w[1118];crq-GAL4,UAS-GFP	
Fig. 3	simu[2]	w[1118];simu[2];crq-GAL4,UAS-GFP	
Fig. 4	control	w[1118];crq-GAL4,UAS-GFP	
Fig. 4	simu[2]	w[1118];simu[2];crq-GAL4,UAS-GFP	
Fig. 5a	apoliner	w[1118];+CyO hs-hid/+da-GAL4,UAS-apoliner	UAS-apoliner obtained from Jean-Paul Vincent, Crick Institute
Fig. 5b	cDOP-1	w[1118];+CyO hs-hid	
Fig. 5c-f	control	w[1118];srp-GAL4,UAS-GFP/CyO	CyO hs-hid obtained from Martin Zeidler, University of Sheffield
Fig. 5c-f	hs-hid	w[1118];srp-GAL4,UAS-GFP/CyO hs-hid	
Fig. 6	control	w[1118];crq-GAL4,UAS-GFP	
Fig. 6	DI(3L)H99	w[1118];DI(3L)H99,crq-GAL4,UAS-GFP	
Fig. 6	simu[2]	w[1118];simu[2];crq-GAL4,UAS-GFP	
Fig. 6	simu[2];DI(3L)H99	w[1118];simu[2];DI(3L)H99,crq-GAL4,UAS-GFP	
Fig. 7a-d	control	w[1118];crq-GAL4,UAS-GFP	
Fig. 7a-b, e-f	simu[2];DI(3L)H99	w[1118];simu[2];DI(3L)H99,crq-GAL4,UAS-GFP	
Fig. 7b, e-f	DI(3L)H99	w[1118];DI(3L)H99,crq-GAL4,UAS-GFP	
Fig. 7b	simu[2]	w[1118];simu[2];crq-GAL4,UAS-GFP	
Supplementary Fig. 1a, c-e	control	w[1118];crq-GAL4,UAS-CD4-tdTomato	
Supplementary Fig. 1b-e	simu[2]	w[1118];simu[2];crq-GAL4,UAS-CD4-tdTomato	
Supplementary Fig. 1f, h-i	control	w[1118];da-GAL4,UAS-GCamp6M	da-GAL4 and UAS-GCamp6M obtained from Alex Whitworth, University of Cambridge and Bloomington, respectively
Supplementary Fig. 1g-i	simu[2]	w[1118];simu[2];da-GAL4,UAS-GCamp6M	
Supplementary Fig. 1j-k	control	w[1118];crq-GAL4,UAS-GFP	
Supplementary Fig. 1j-k	simu[2]/+	w[1118];simu[2]/+crq-GAL4,UAS-GFP	
Supplementary Fig. 1j-k	DI(2L)BSC253/+	w[1118];DI(2L)BSC253/+crq-GAL4,UAS-GFP	DI(2L)BSC253 obtained from Bloomington Stock Centre
Supplementary Fig. 1j-k	simu[2];DI(2L)BSC253	w[1118];DI(2L)BSC253/simu[2];crq-GAL4,UAS-GFP	
Supplementary Fig. 1l-m	control	w[1118];srp-GAL4,UAS-red slinger/+crq-GAL4,UAS-GFP/+	UAS-red slinger obtained from Brian Stramer, KCL
Supplementary Fig. 1l-m	simu[2]	w[1118];simu[2];srp-GAL4,UAS-red slinger/simu[2];crq-GAL4,UAS-GFP/UAS-simu	UAS-simu obtained from Estee Kurant, University of Haifa
Supplementary Fig. 1l-m	srp, crq>simu	w[1118];srp-GAL4,UAS-red slinger/+crq-GAL4,UAS-GFP/UAS-simu	
Supplementary Fig. 1l-m	simu[2];srp, crq>simu	w[1118];simu[2];srp-GAL4,UAS-red slinger/simu[2];crq-GAL4,UAS-GFP/UAS-simu	
Supplementary Fig. S2a-d	control	w[1118];+CyO hs-hid/+da-GAL4,UAS-apoliner	
Supplementary Fig. S2e	control	w[1118];srp-GAL4,UAS-GFP/CyO	
Supplementary Fig. S2e	hs-hid	w[1118];srp-GAL4,UAS-GFP/CyO hs-hid	
Supplementary Fig. S2f-g	srp-GAL4,UAS-GFP/+	w[1118];srp-GAL4,UAS-GFP/+	
Supplementary Fig. S2f-g	srp-GAL4,UAS-GFP/CyO	w[1118];srp-GAL4,UAS-GFP/CyO	
Supplementary Fig. S2f-g	srp-GAL4,UAS-GFP/CyO hs-hid	w[1118];srp-GAL4,UAS-GFP/CyO hs-hid	



Supplementary Fig. 3a-d	control	w1118];crq-GAL4,UAS-GFP	
Supplementary movie 1	control	w1118];crq-GAL4,UAS-GFP	
Supplementary movie 1	simu[2]	w1118];simu[2];crq-GAL4,UAS-GFP	
Supplementary movie 2	control	w1118];crq-GAL4,UAS-GFP	
Supplementary movie 2	simu[2]	w1118];simu[2];crq-GAL4,UAS-GFP	
Supplementary movie 3	control	w1118];+CyO hs-hid;+da-GAL4,UAS-apoliner	
Supplementary movie 4	control	w1118];srp-GAL4,UAS-GFP/CyO	
Supplementary movie 4	hs-hid	w1118];srp-GAL4,UAS-GFP/CyO hs-hid	
Supplementary movie 5 and 6	control	w1118];crq-GAL4,UAS-GFP	
Supplementary movie 5 and 6	D[3L]H99	w1118];D[3L]H99;crq-GAL4,UAS-GFP	
Supplementary movie 5 and 6	simu[2]	w1118];simu[2];crq-GAL4,UAS-GFP	
Supplementary movie 5 and 6	simu[2];D[3L]H99	w1118];simu[2];D[3L]H99;crq-GAL4,UAS-GFP	
Supplementary movie 7	control	w1118];crq-GAL4,UAS-GFP	
Supplementary movie 7	simu[2];D[3L]H99	w1118];simu[2];D[3L]H99;crq-GAL4,UAS-GFP	
Supplementary movie 8	control	w1118];crq-GAL4,UAS-GFP	

## Supplementary movies

### Supplementary movie 1 – Macrophages migrate at slower speeds in *simu* mutants compared to controls

30-minute movies of GFP-labelled macrophages at stage 15 on the ventral midline showing their random migration in control (*w;;crq-GAL4,UAS-GFP*, upper embryo) and *simu* mutant embryos (*w;simu<sup>2</sup>;crq-GAL4,UAS-GFP*, lower embryo). Movies repeat with second movie showing tracks of macrophage migration. Scale bar represents 20µm.

### Supplementary movie 2 – Macrophage responses to wounds are perturbed in *simu* mutant embryos

Movies of the inflammatory migration of GFP-labelled macrophages to epithelial wounds in control (*w;;crq-GAL4,UAS-GFP*, embryo on left) and *simu* mutant embryos (*w;simu<sup>2</sup>;crq-GAL4,UAS-GFP*, embryo on right) at stage 15 of development on the ventral midline. Embryos wounded in the centre of the field of view. Scale bar represents 25µm.

### Supplementary movie 3 - Induction of apoptosis visualised using the apoliner caspase reporter

Movie of *w;CyO hs-hid/+;da-GAL4,UAS-apoliner/+* embryos heat-shocked for 0 minutes (negative control), 5 minutes, 15 minutes, 30 minutes and 60 minutes; time-lapse movies begin 1-hour post-heat shock. Caspase activity results in cleavage of apoliner, enabling its nls-GFP to translocate to the nucleus, whereas CD8-RFP remains on membranes. Caspase activity increases rapidly from 1-hour post-heat shock, with the majority of caspase-positive cells remaining in an intact epithelium beyond the period of time in which inflammatory responses are typically followed. Movie shows green channel in first instance; second cycle shows merged image with GFP in green and RFP in purple. Scale bar represents 50µm.

### Supplementary movie 4 - Exogenous apoptosis impairs inflammatory responses of macrophages

Movies of GFP-labelled macrophage migration to wounds in a control embryo (*w;srp-GAL4,UAS-GFP/CyO*) and an embryo in which exogenous apoptosis has been introduced through Hid expression (*w;srp-GAL4,UAS-GFP/CyO hs-hid*). Both embryos were heat-shocked for 15 minutes, with laser-wounding taking place 1-hour post heat-shock at a time-point when caspase activity is dramatically increasing, but when engulfment of cells destined to die has yet to take place. Fewer macrophages migrate to wounds in the presence of apoptotic cells, suggesting that apoptosis, but not necessarily phagocytosis of dying cells,

can dampen inflammatory responses. Dotted lines show wound sites; scale bar represents 20µm.

### Supplementary movie 5 - Rescue of wandering migration in *simu* mutants with no apoptosis

Hour-long movies of GFP-labelled macrophages in control (*w;;crq-GAL4,UAS-GFP*), apoptosis-null *Df(3L)H99* mutant (*w;;Df(3L)H99,crq-GAL4,UAS-GFP*), *simu* mutant (*w;simu<sup>2</sup>;crq-GAL4,UAS-GFP*) and apoptosis-null *simu* mutant embryos (*w;simu<sup>2</sup>;Df(3L)H99,crq-GAL4,UAS-GFP*) at stage 15. Removal of apoptotic cell death rescues macrophage speeds in a *simu* mutant background. Note the absence of vacuoles in *Df(3L)H99* and *simu<sup>2</sup>;Df(3L)H99* embryos due to the lack of apoptotic cell death. Scale bar represents 20µm.

### Supplementary movie 6 - Rescued initial responses to wounds in the absence of apoptosis in *simu* mutants

Hour-long movies of GFP-labelled macrophages in control (*w;;crq-GAL4,UAS-GFP*), apoptosis-null *Df(3L)H99* mutant (*w;;Df(3L)H99,crq-GAL4,UAS-GFP*), *simu* mutant (*w;simu<sup>2</sup>;crq-GAL4,UAS-GFP*) and apoptosis-null *simu* mutant embryos (*w;simu<sup>2</sup>;Df(3L)H99,crq-GAL4,UAS-GFP*) at stage 15 following wounding; initial image shows pre-wound image. Removal of apoptotic cell death rescues the percentage of macrophages responding to wounds in a *simu* mutant background. Note the absence of vacuoles in *Df(3L)H99* and *simu<sup>2</sup>;Df(3L)H99* embryos due to the lack of apoptotic cell death. Scale bar represents 20µm.

### Supplementary movie 7 - Enhanced macrophage resolution from wounds in the absence of *simu*

Movies of GFP-labelled macrophages during wound responses to laser-induced epithelial wounds on the ventral midline in a control embryo (*w;;crq-GAL4,UAS-GFP*; embryo on left) and *simu* mutant that lacks apoptosis (*w;simu<sup>2</sup>;Df(3L)H99,crq-GAL4,UAS-GFP*; embryo on right). First repeat of wound response shows GFP channel only; second repetition shows all tracks of those cells present at 0-minutes post-wounding superimposed over GFP channel; third repetition shows tracks of macrophages that leave the wound (1 cell in control embryo, 5 cells in the *simu<sup>2</sup>;Df(3L)H99* embryo). Scale bar represents 20µm.

### Supplementary movie 8 - Macrophages interact with annexin V-labelled debris at wounds

Movie showing accumulation of annexin V to label exposed phosphatidylserine (PS) at wounds during an inflammatory response in a control embryo (*w;;crq-GAL4,UAS-GFP*). Initial run of time-lapse movie shows texas red-labelled annexin V alone, second repeat

shows GFP-labelled macrophages (green) and annexin V (purple). Injection of fluorescent annexin V into the vitelline space labels the wound edge, suggesting that PS decorates stressed or damaged cells at these sites. Scale bar represents 20 $\mu$ m.